Article

Discovery Medicine 2024; 36(186): 1486–1498
https://doi.org/10.24976/Discov.Med.202436186.138

Knockdown of YAP1 Reduces YTHDF3 to Stabilize *SMAD7* and thus Inhibit Bladder Cancer Stem Cell Stemness

Dandan Qiu[1], Lingling Gao[2], Xingwei Yu[1,*]

[1]Department of Urology, The First Affiliated Hospital of Zhejiang Chinese Medical University (Zhejiang Provincial Hospital of Chinese Medicine), 310000 Hangzhou, Zhejiang, China
[2]Department of Urology, The First Affiliated Hospital of Zhejiang University, 310009 Hangzhou, Zhejiang, China
*Correspondence: xingweiyu@126.com (Xingwei Yu)
Published: 20 July 2024

Background: The previous study has proved the oncogenic role of Yes-associated protein 1 (YAP1) in bladder cancer (BLCA), thus this study focused on its impact on bladder cancer stem cells (BCSCs) and underlying mechanism.
Method: BCSCs were obtained by treating human BLCA cells UMUC3 with cisplatin and identified by measuring CD133$^+$ in UMUC3/BCSCs via flow cytometry. YAP1 interaction proteins and mothers against decapentaplegic homolog 7 (*SMAD7*) N6-methyladenosine (m6A) site were analyzed by bioinformatics. BCSCs were transfected. *SMAD7* m6A level, YTH domain-containing family proteins 3 (YTHDF3)-*SMAD7* interaction, YAP1/YTHDF3 expression in BCSCs were assessed by methylated RNA immunoprecipitation (MeRIP), RNA immunoprecipitation (RIP) or quantitative reverse transcription PCR (qRT-PCR), respectively. BCSC proliferation was detected by 5-Bromo-2-deoxyuridine (BrdU) staining. UMUC3/BCSC migration/invasion and tumour sphere formation were determined by Transwell or tumour sphere formation assays. YAP1/YTHDF3/*SMAD7*/transforming growth factor (TGF)-β1/stemness marker expressions in UMUC3/BCSCs were measured by Western blot assay.
Result: BCSCs showed higher CD133$^+$ ratio, expressions of stemness marker/YAP1/YTHDF3/TGF-β1, lower *SMAD7* expression and greater invasion/migration/tumour sphere formation capabilities than UMUC3 cells. YAP1 knockdown decreased *SMAD7* m6A level and impaired YTHDF3-*SMAD7* interaction in BCSCs. YAP1 silencing inhibited cell growth/invasiveness/migration/tumour sphere formation and stemness-associated protein/YTHDF3/TGF-β1 expressions while upregulating *SMAD7* expression in BCSCs, which was offset by YTHDF3 overexpression.
Conclusion: The silencing of YAP1 in BCSCs impedes the YTHDF3-mediated degradation of m6A-modified *SMAD7*, culminating in diminished cell stemness.

Keywords: YAP1; YTHDF3; *SMAD7*; stemness; bladder cancer; m6A methylation

Introduction

Bladder cancer (BLCA) stands as a prevalent urinary malignancy marked by heightened incidence rates, widespread prevalence, mortality, and substantial medical costs, constituting a significant health burden [1,2]. The primary treatment for BLCA remains transurethral cystectomy with bladder preservation, yet it is susceptible to postoperative recurrence. Additional therapeutic modalities predominantly involve systemic approaches centered on cisplatin-based regimens; however, chemotherapy is associated with numerous adverse reactions, limited patient tolerance, and susceptibility to drug resistance [3]. Hence, the exploration of novel therapeutic avenues against BLCA is imperative to achieve improved outcomes.

Cancer stem cells (CSCs), characterized by undifferentiated cells with stem-like properties, significantly contribute to the high recurrence rate of BLCA, thereby emerging as potential targets in BLCA treatment [4]. The stemness phenotype serves as a hallmark of tumor progression, with increased stemness observed during BLCA development [5]. N6-methyladenosine (m6A) modification, known to regulate stemness properties across various cancers, including BLCA, serves as an indicator for cancer diagnosis, treatment, and prognosis [6]. The m6A "reader" protein YTH domain-containing family protein 3 (YTHDF3) plays a crucial role in mRNA translation or degradation [7], and its involvement in BLCA progression through mRNA modification has been documented [8].

Yes-associated protein 1 (YAP1) serves as a transcriptional co-activator involved in various cellular processes including proliferation, migration, differentiation and apoptosis [9]. Elevated YAP1 expression in BLCA correlates with poorer prognosis and overall survival rates among patients,

while also driving cancer progression through the promotion of epithelial-mesenchymal transition (EMT) of tumour cells [10]. Activation of EMT has been shown to induce tumorigenicity and stemness in BLCA [11]. Furthermore, YAP1 is implicated in m6A modification, as it regulates the expression levels of m6A modulators, leading to increased gene methylation levels [12]. These findings suggest a potential relationship between YAP1 and the stemness phenotype of BLCA through m6A modification.

Interactive genes of YAP1, cancer stemness and BLCA, mothers against decapentaplegic homolog 7 (*SMAD7*) were selected for the investigation of YAP1 mechanisms in this study and m6A sites of *SMAD7* were obtained from the RMBase database. *SMAD7* is an antagonist of the transforming growth factor (TGF)-β signaling [13], which plays a promoting role in cancer development by facilitating the EMT of cancer cells [14]. In BLCA, overexpression of *SMAD7* negatively regulated EMT to restrain tumour metastasis [15]. Evidence has revealed the inverse correlation between *SMAD7* and YAP1 in liver cancer [16]. In addition, *SMAD7* mRNA expression is negatively controlled by m6A modulator methyltransferase-like 3 (*METTL3*) [17], while YTHDF3 is involved in the regulation of *METTL3*-modified gene expression [18]. Since YAP1 has been demonstrated to upregulate YTHDF3 level to induce gene degradation [19], it may also affect *SMAD7* expression via YTHDF3.

Based on these findings, we assumed that YAP1 contributes to BLCA stemness by regulating the expression of m6A-methylated *SMAD7* via YTHDF3.

Materials and Methods

Cell Culture and Induction

The human BLCA cell line UMUC3 (CL-0463, Procell, Wuhan, China) was cultured in Minimum Essential Medium (MEM, PM150410, Procell, Wuhan, China), supplemented with Non-Essential Amino Acids (NEAA), 10% Fetal Bovine Serum (FBS, C0227, Beyotime, Shanghai, China), and 1% Penicillin-Streptomycin Solution (PB180120, Procell, Wuhan, China). Cultures were maintained at 37 °C in a 5% CO_2 atmosphere in an incubator (E3293, Beyotime, Shanghai, China). To isolate bladder cancer stem cells (BCSCs), UMUC3 cells were subjected to daily treatment with 6.66 µM cisplatin (PHR1624, Merck, Darmstadt, Germany) for 90 days, followed by treatment with 13.32 µM cisplatin/day for an additional 14 days [20]. Prior to experiments, all cells underwent routine STR identification and mycoplasma contamination tests to confirm absence of mycoplasma contamination.

Flow Cytometry

To isolate $CD133^+$ cells, 1×10^5 BCSCs/UMUC3 cells were blocked with 1% Bovine Serum Albumin (BSA, 10711454001, Roche, Basel, Switzerland) for 20 minutes. Subsequently, cells were incubated with PE-conjugated anti-CD133 antibody (ab252128, 1:1000, Abcam, London, UK) at 4 °C for 1 hour (h). The proportion of $CD133^+$ cells was determined using a FACSCalibur flow cytometer (BECKMAN COULTER, Brea, CA, USA).

Bioinformatic Analysis

The protein-protein interaction (PPI) network of YAP1 was retrieved from the STRING database (https://cn.string-db.org/).

Transfection

Short hairpin RNA targeting *YAP1* (Sh*YAP1*, TR308332, CCACCAAGCTAGATAAAGAAA) and negative control pRS vector (ShNC, TR20003), as well as the YTHDF3 overexpression plasmid (RC208423) and its negative control pCMV6-Entry vector (PS100001), were procured from OriGene Technologies (Rockville, MD, USA). The coding sequence (CDS) of the *YAP1* gene is provided in the **Supplementary Materials**. BCSCs were transfected with ShNC/NC/Sh*YAP1*/YTHDF3 overexpression plasmid or co-transfected with ShNC plus NC/Sh*YAP1* plus YTHDF3 overexpression plasmid using Lipofectamine™ 3000 Transfection Reagent (L3000008, ThermoFisher, Waltham, MA, USA). A total of 1×10^6 BCSCs were seeded into 96-well plates and cultured until reaching 90% confluence. DNA (0.2 µg) was diluted in 10 µL of serum-free medium and mixed with 0.4 µL of P3000 Reagent, while ShRNA was diluted in serum-free medium. Subsequently, 5 µL of DNA/ShRNA was incubated with 5 µL of diluted Lipofectamine™ 3000 Reagent for 15 min at room temperature. The resulting complex was then added to the cells and incubated at 37 °C for 48 h.

Methylated RNA Immunoprecipitation (MeRIP)

An N6-methyladenosine (*m6A*) MeRIP Kit (GS-ET-001, CloudSeq, Shanghai, China, http://www.cloud-seq.com.cn/) was utilized to detect *SMAD7* m6A levels. Total RNA was extracted from normal/ShNC-/Sh*YAP1*-transfected BCSCs using a PureLink RNA Mini Kit (12183018A, ThermoFisher, Waltham, MA, USA). The isolated total RNA was dissolved in RNase-free water, purified with ethanol, and subsequently fragmented to approximately 200 nucleotides in length. RNA concentration was measured using an RNA 6000 Pico kit (5067-1513, Agilent, Santa Clara, CA, USA).

Protein A/G beads (25 µL) were incubated with 2 µL of anti-m6A antibody (ab286164, Abcam, London, UK) or control Rabbit Anti-Human Immunoglobulin G (IgG, ab6715, Abcam, London, UK) on a shaker for 1 h at room temperature to allow for antibody conjugation. Subsequently, the fragmented RNAs (3 µg) were mixed with RNase-free water and IP buffer (50 µL) to prepare the MeRIP reaction mixture (250 µL). The antibody-conjugated beads were then incubated with the MeRIP re-

action mixture (250 µL) for 1 h at 4 °C to immunoprecipitate *m6A*-RNA complexes. Following immunoprecipitation, the complexes were eluted from the beads, purified, and subjected to quantitative reverse transcription PCR (qRT-PCR) to measure the level of *SMAD7*. Results were calculated as *SMAD7* level/Input.

RNA Immunoprecipitation (RIP)

The interaction between YTHDF3 and *SMAD7* in untreated/ShNC-/Sh*YAP1*-transfected BCSCs was assessed using a Magna RIP kit (17-704, Sigma-Aldrich, Darmstadt, Germany). A total of 2×10^6 BCSCs were lysed with Lysis Buffer and centrifuged at 40,000 ×g for 10 min at 4 °C to obtain the cell lysate. Protein A/G magnetic beads were then incubated with 5 µg of anti-YTHDF3 antibody (ab220161, Abcam, London, UK) or IgG for 1 h at room temperature to facilitate antibody conjugation. Subsequently, the antibody-conjugated beads were incubated with 800 µL of the cell lysate overnight at 4 °C to immunoprecipitate YTHDF3-RNA complexes.

Following immunoprecipitation, the complexes were eluted from the beads, purified, and the expression of *SMAD7* within the complexes was measured using qRT-PCR.

Quantitative Reverse Transcription PCR (qRT-PCR)

RNA extraction from normal/transfected BCSCs was performed as previously described, followed by cDNA synthesis using a PrimeScript™ Kit (6210A, TaKaRa, Shiga, Japan). qRT-PCR was conducted using PowerUp™ SYBR™ Green Master Mix (A25742, Applied Biosystems, Foster, CA, USA) on the LightCycler® 96 System (05815916001, Roche, Basel, Switzerland). The amplification conditions were set as follows: 97 °C for 15 s, followed by 30 cycles at 90 °C for 5 s, 60 °C for 40 s, and 72 °C for 1 min. RNA expression levels were calculated using the $2^{-\Delta\Delta CT}$ method and normalized to glyceraldehyde-3-phosphate dehydrogenase (*GAPDH*). The primer sequences used were as follows:

SMAD7 (*m6A*):
Forward (F): 5′-GTCCGAATTGAGCTGTCCGA-3′;
Reverse (R): 5′-AACCCTCTCTGCCAATGTGT-3′.
SMAD7:
F: 5′-CAGCGGCCCAAUGACCACGAGUUUA-3′;
R: 5′-UAAACUCGUGGUCAUUGGGCCGCUG-3′.
YAP1:
F: 5′-TAGCCCTGCGTAGCCAGTTA-3′;
R: 5′-TCATGCTTAGTCCACTGTCTGT-3′.
YTHDF3:
F: 5′-TCAGAGTAACAGCTATCCACCA-3′;
R: 5′-GGTTGTCAGATATGGCATAGGCT-3′.
GAPDH:
F: 5′-AGCTGAACGGGAAGCTCACT-3′;
R: 5′-TGCTTAGCCAAATTCGTTG-3′.

5-Bromo-2-Deoxyuridine (BrdU) Staining

Transfected BCSCs (5×10^3 cells) were seeded onto 24-well plates supplemented with 10 µM BrdU labeling solution (ab142567, Abcam, London, UK) and incubated for 24 h at 37 °C with 5% CO_2. Following incubation, the BrdU labeling solution was removed, and the cells were washed thrice with PBS Tween-20 (28352, ThermoFisher, Waltham, MA, USA). Subsequently, the cells were treated with 2.5 M HCL at room temperature for 1 h for DNA hydrolysis. Afterward, the cells were fixed in 4% paraformaldehyde (P1110, Solarbio, Beijing, China), permeabilized with 0.3% Triton-X-100 (HFH10, ThermoFisher, Waltham, MA, USA), and blocked with 5% BSA at room temperature for 1 h.

Next, BCSCs were incubated with anti-BrdU antibody (ab6326, 1:100, Abcam, London, UK) overnight at 4 °C. Following three washes with PBS Tween-20, Alexa Fluor® 488-conjugated goat anti-rat IgG (ab150165, 1:300, Abcam, London, UK) was added for cell incubation at room temperature for 1 h. The cell nuclei were counterstained with 4′,6-diamidino-2-phenylindole (DAPI, D3571, ThermoFisher, Waltham, MA, USA). BrdU-positive cells were counted under the field of a fluorescence microscope (TE2000, Nikon, Tokyo, Japan).

Transwell Assay

For cell migration detection, HTS 24-well insert plates (354144, Corning Life Sciences, Corning, NY, USA) were employed, while 24-well Matrigel-precoated BioCoat™ cell culture inserts (354480, Corning Life Sciences, Corning, NY, USA) were utilized for cell invasion analysis. UMUC3 cells and normal/transfected BCSCs (1×10^4) were trypsinized and plated in 600 µL serum-free culture medium on the Matrigel-coated upper chamber, while the lower chamber was filled with 600 µL complete culture medium with 10% FBS.

After a 24-h incubation period at 37 °C, cells attached to the upper surface of the membrane were removed and the migrated/invaded cells on the lower surface were stained with 0.1% crystal violet (C0121, Beyotime, Shanghai, China) and observed under a BX51 light microscope (OLYMPUS, Tokyo, Japan) (magnification × 250, scale bar = 50 µm).

Tumour Sphere Formation

UMUC3 cells/BCSCs, with or without transfection, were cultured in 24-well plates at a density of 5000 cells per well. The culture medium consisted of serum-free RPMI-1640 (PM150110, Procell, Wuhan, China), supplemented with 20 ng/mL fibroblast growth factor (FGF, F0291, Merck, Darmstadt, Germany), epidermal growth factor (EGF, E9644, Sigma-Aldrich, Darmstadt, Germany), 5 µg/mL insulin (I9278, Sigma-Aldrich, Darmstadt, Germany), and 2% B27 (a1486701, Gibco, Grand Island, NY, USA). Cultures were maintained for 7 days. Tumor spheres

were visualized using a BX51 microscope (OLYMPUS, Tokyo, Japan) (magnification × 200, scale bar = 100 µm) [21].

Western Blot Assay

Total proteins were extracted from normal UMUC3/BCSCs and transfected BCSCs using the Minute™ Total Protein Extraction Kit (SD-001/SN-002, Invent Biotechnologies, Eden Prairie, MN, USA) and quantified using a Quick Start Bradford assay kit (5000201, Bio-Rad, Hercules, CA, USA). Protein separation was carried out using SDS-PAGE Hepes Electrophoresis Buffer (P0552, Beyotime, Shanghai, China), and the isolated proteins were loaded onto Polyvinylidene Fluoride (PVDF) membranes (03010040001, Roche, Basel, Switzerland). Subsequently, the membranes were blocked with 5% skim milk at room temperature for 1 h.

Thereafter, the blocked membranes were reacted with primary antibody against YAP1 (ab52771, 1:5000, 72 kDa, Abcam, London, UK), YTHDF3 (ab220161, 1:1000, 73 kDa, Abcam, London, UK), SMAD7 (ab216428, 1:1000, 46 kDa, Abcam, London, UK), TGF-β1 (ab215715, 1:1000, 44 kDa, Abcam, London, UK), CD133 (ab222782, 1:2000, 97 kDa, Abcam, London, UK), octamer-binding transcription factor 4 (Oct-4, ab181557, 1:1000, 45 kDa, Abcam, London, UK), Nanog (ab109250, 1:1000, 37 kDa, Abcam, London, UK) or internal control GAPDH (ab9485, 1:2500, 37 kDa, Abcam, London, UK) at 4 °C overnight, followed by 1-h incubation with secondary antibody Goat Anti-Rabbit IgG (ab205718, 1:2000, Abcam, London, UK). Blots were visualized using the Chemiluminescence HRP Substrate (T7101Q, TaKaRa, Shiga, Japan) and detected by TotalLab TL 120 software (Nonlinear Dynamics Ltd., Newcastle, UK).

Statistical Analysis

Statistical analysis was conducted using GraphPad Prism 8.0 software (GraphPad, San Diego, CA, USA). Measurement data were expressed as mean ± standard deviation (SD). One-way Analysis of Variance (ANOVA) was utilized for comparisons among multiple groups, while an independent sample *t*-test was employed for comparisons between two groups, with the post-hoc analysis of Tukey test. In addition, the normality is tested using Shapiro Wilk test, and the homogeneity of variance is tested using Levene test. A *p*-value less than 0.05 was considered statistically significant.

Results

BCSCs Exhibited High Stemness and Capabilities of Migration, Invasion and Tumour Sphere Formation

A higher proportion of $CD133^+$ cells was observed in BCSCs compared to UMUC3 cells (Fig. 1A,B, $p < 0.001$). Furthermore, levels of stemness markers CD133, Oct-4, and Nanog were elevated in BCSCs compared to UMUC3 cells (Fig. 1C,D, $p < 0.01$). The Transwell assay revealed that BCSCs exhibited stronger migration and invasion activities than UMUC3 cells (Fig. 1E–G, $p < 0.001$). Moreover, the quantity of tumor spheres formed by BCSCs was significantly greater than that observed in UMUC3 cells (Fig. 1H,I, $p < 0.001$).

YAP1-Interacting Protein SMAD7 was Lowly Expressed in BCSCs while YAP1, YTHDF3 and TGF-β1 were Highly Expressed in BCSCs

The PPI network depicted interacting proteins of YAP1 (Fig. 2A). Results from the Western blot assay revealed elevated levels of YAP1, YTHDF3, and TGF-β1 proteins, along with decreased levels of SMAD7 protein in BCSCs compared to UMUC3 cells (Fig. 2B,C, $p < 0.001$).

Knockdown of YAP1 Inhibited the Proliferation, Migration and Invasion Abilities and Decreased Stemness-Related Protein Levels in BCSCs

Silencing of *YAP1* in BCSCs resulted in decreased *YAP1* mRNA expression (Fig. 3A, $p < 0.001$). BCSC proliferation was inhibited by Sh*YAP1* (Fig. 3B,C, $p < 0.001$). Furthermore, YAP1 inhibition in BCSCs reduced CD133, Oct-4, and Nanog protein levels (Fig. 3D–G, $p < 0.01$). Following the transfection of Sh*YAP1* in BCSCs, a significant decrease in cell migration and invasion rates was observed (Fig. 3H–J, $p < 0.001$).

YAP1 Knockdown Restrained Tumour Sphere Formation as well as YAP1, YTHDF3 and TGF-β1 Expression Levels while Increasing SMAD7 Expression in BCSCs

Inhibition of YAP1 resulted in a decrease in the number of tumor spheres in BCSCs (Fig. 4A,B, $p < 0.001$). Protein levels of YAP1, YTHDF3, and TGF-β1 all decreased, while that of *SMAD7* increased in Sh*YAP1*-transfected BCSCs (Fig. 4C,D, $p < 0.001$).

Inhibition of YAP1 Decreased SMAD7 m6A Level and Impaired YTHDF3-SMAD7 Interaction in BCSCs

The level of m6A-modified *SMAD7* was decreased in YAP1-underexpressing BCSCs, as compared with that in ShNC-transfected BCSCs (Fig. 4E, $p < 0.001$). RIP assay showed that compared with IgG, anti-YTHDF3 antibody induced the enrichment of *SMAD7* RNA at a higher level from normal BCSCs, ShNC-transfected BCSCs and YAP1-underexpressing BCSCs (Fig. 4F, $p < 0.001$), which indicated that YTHDF3 bound to *SMAD7*. Furthermore, YAP1 silencing relative to shNC transfection in BCSCs led to an increased *SMAD7* level in the Input group (Fig. 4F, $p < 0.05$), but resulted in a decreased level of *SMAD7* RNA enriched by anti-YTHDF3 antibody (Fig. 4F, $p < 0.001$), suggesting that the interaction between YTHDF3 and *SMAD7*

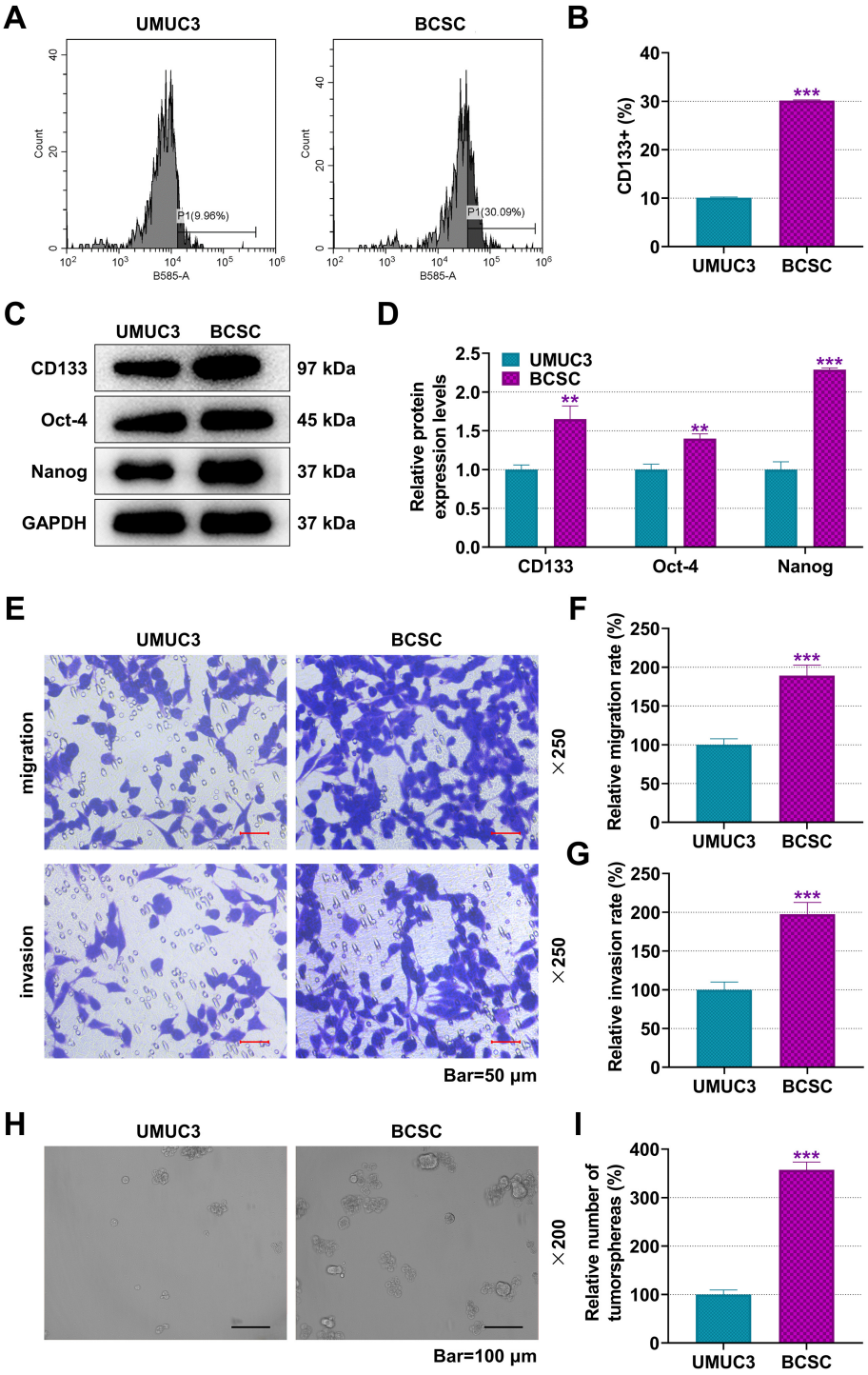

Fig. 1. BCSCs exhibited high stemness and capabilities of migration, invasion and tumour sphere formation. (A,B) The proportion of $CD133^{+}$ cells in UMUC3/BCSCs was detected by flow cytometry. (C,D) Western blot assay was performed to assess CD133, Oct-4 and Nanog protein expression levels in UMUC3/BCSCs, with glyceraldehyde-3-phosphate dehydrogenase (GAPDH) as the loading control. (E–G) The invasive/migratory activities of UMUC3/BCSCs were assessed by Transwell assay (magnification × 250, scale bar = 50 μm). (H,I) Images of tumour spheres (magnification × 200, scale bar = 100 μm). The number of tumour spheres in UMUC3/BCSCs was observed by microscope. BCSCs: UMUC3 cells incubated with 6.66 μM cisplatin/day for 19 days and 13.32 μM cisplatin/day for 14 days. BCSCs, bladder cancer stem cells; Oct-4, octamer-binding transcription factor 4. *vs. UMUC3: $^{***}p < 0.001$, $^{**}p < 0.01$. n = 3.

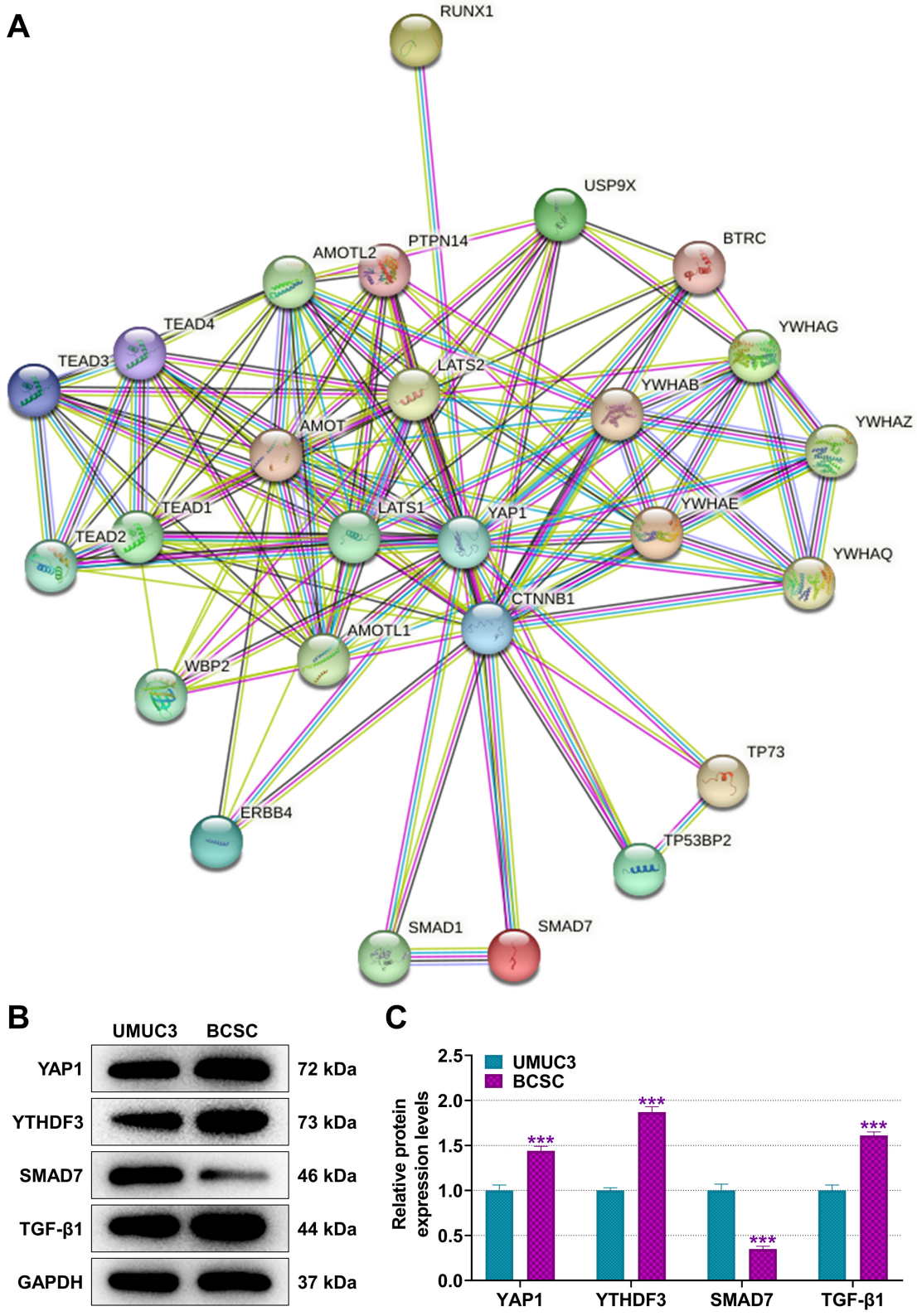

Fig. 2. YAP1-interacting protein SMAD7 was downregulated in BCSCs while YAP1, YTHDF3 and TGF-β1 levels were upregulated in BCSCs. (A) The PPI network of YAP1 was obtained from the STRING database (https://cn.string-db.org/). (B,C) Protein levels of YAP1/YTHDF3/SMAD7/TGF-β1 in UMUC3/BCSCs were measured by Western blot and normalized to GAPDH. BCSCs: UMUC3 cells incubated with 6.66 µM cisplatin/day for 19 days and 13.32 µM cisplatin/day for 14 days. PPI, protein-protein interaction; YAP1, Yes-associated protein 1; YTHDF3, YTH domain-containing family proteins 3; SMAD7, mothers against decapentaplegic homolog 7; TGF-β1, transforming growth factor-β1. *vs. UMUC3: $^{***}p < 0.001$. n = 3.

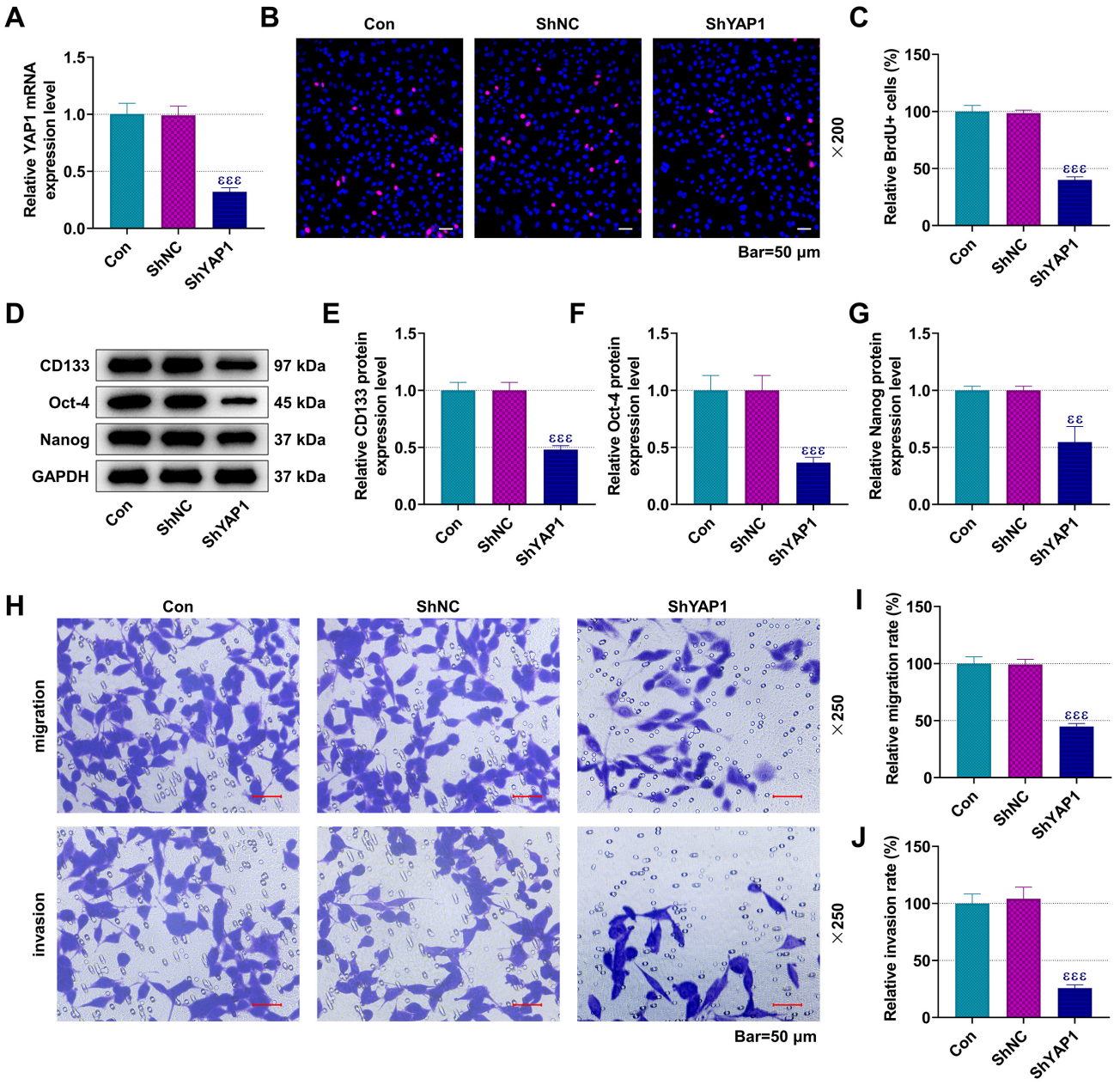

Fig. 3. Knockdown of *YAP1* inhibited the proliferation, migration and invasion abilities and decreased stemness-related protein levels in BCSCs. (A) *YAP1* mRNA expression in BCSCs was calculated by qRT-PCR and *GAPDH* was used as an internal reference. (B,C) BCSC proliferation ability was assessed by BrdU assay (magnification × 200, scale bar = 50 μm). (D–G) Protein levels of CD133, Oct-4 and Nanog in BCSCs were measured by Western blot assay and normalized to GAPDH. (H–J) Transwell assay was carried out for the analyzing the migration and invasion of BCSCs (magnification × 250, scale bar = 50 μm). Con group: normal BCSCs; ShNC group: ShNC-transfected BCSCs; Sh*YAP1* group: Sh*YAP1*-transfected BCSCs. Con, control; ShNC, short hairpin RNA negative control; Sh*YAP1*, short hairpin RNA targeting *YAP1*; BrdU, 5-Bromo-2-deoxyuridine; qRT-PCR, quantitative reverse transcription PCR. $^{\varepsilon}$vs. ShNC: $^{\varepsilon\varepsilon\varepsilon}p < 0.001$, $^{\varepsilon\varepsilon}p < 0.01$. n = 3.

was disrupted in BCSCs after the inhibition of YAP1, and this severed interaction however increased in the expression of *SMAD7* RNA. Overall, the above results implied that knockdown of YAP1 may reduce m6A modification at *SMAD7* to prevent YTHDF3-mediated decay of m6A-modified *SMAD7*.

YAP1 Knockdown-Induced Inhibition on Cell Growth/Migration/Invasion/Stemness Maker Expression Levels in BCSCs was Reversed by YTHDF3 Overexpression

YTHDF3 mRNA levels in BCSCs were enhanced by YTHDF3 overexpression (Fig. 5A, $p < 0.001$). This overexpression effectively reversed the inhibitory effect

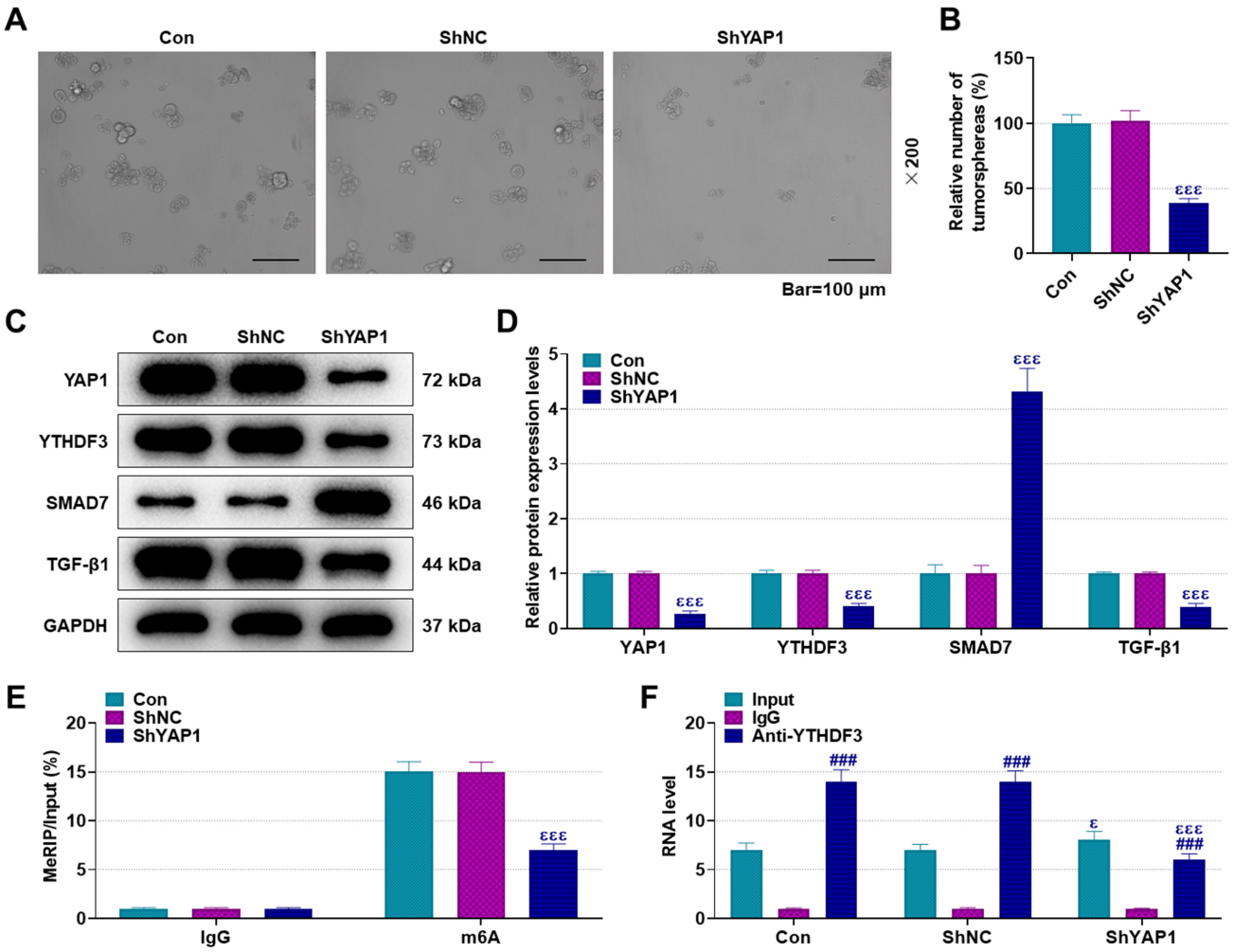

Fig. 4. YAP1 knockdown restrained tumour sphere formation/YAP1, YTHDF3 and TGF-β1 expression levels/*SMAD7* m6A level/YTHDF3-*SMAD7* interaction while increasing *SMAD7* expression in BCSCs. (A,B) Imagines of tumour spheres in BCSCs (magnification × 200, scale bar = 100 μm) and the number of tumor spheres were counted. (C,D) Protein levels of YAP1/YTHDF3/*SMAD7*/TGF-β1 in BCSCs were measured by Western blot assay and normalized to GAPDH. (E) MeRIP was conducted to measure *SMAD7* m6A level in BCSCs. (F) YTHDF3-*SMAD7* interaction was assessed by RIP assay. Con group: normal BCSCs; ShNC group: ShNC-transfected BCSCs; Sh*YAP1* group: Sh*YAP1*-transfected BCSCs. m6A, N6-methyladenosine; MeRIP, methylated RNA immunoprecipitation; IgG, Immunoglobulin G; RIP, RNA immunoprecipitation. $^{\#}$vs. IgG, $^{\varepsilon}$vs. ShNC: $^{\#\#\#}p < 0.001$, $^{\varepsilon\varepsilon\varepsilon}p < 0.001$, $^{\varepsilon}p < 0.05$. n = 3.

of YAP1 knockdown on BCSC proliferation activities (Fig. 5B,C, $p < 0.001$). The suppressive effects of YAP1 silencing on CD133, Oct-4, and Nanog protein expression levels in BCSCs were counteracted by YTHDF3 overexpression (Fig. 5D–G, $p < 0.001$). Furthermore, YTHDF3 overexpression also mitigated the YAP1 knockdown-induced impairment of BCSC migration and invasion capabilities (Fig. 5H–J, $p < 0.001$).

Effects of YAP1 Knockdown on Tumour Sphere Formation as well as YTHDF3, TGF-β1 and SMAD7 Expression Levels in BCSCs were Negated by YTHDF3 Overexpression

YTHDF3 overexpression attenuated the YAP1 knockdown-induced repression of tumor sphere formation ability in BCSCs (Fig. 6A,B, $p < 0.001$). Western blot assay demonstrated that the YAP knockdown-induced inhibition of YTHDF3 and TGF-β1 expression levels, as well as the stimulation of *SMAD7* expression in BCSCs, was reversed by YTHDF3 overexpression (Fig. 6C,D, $p <$ 0.001).

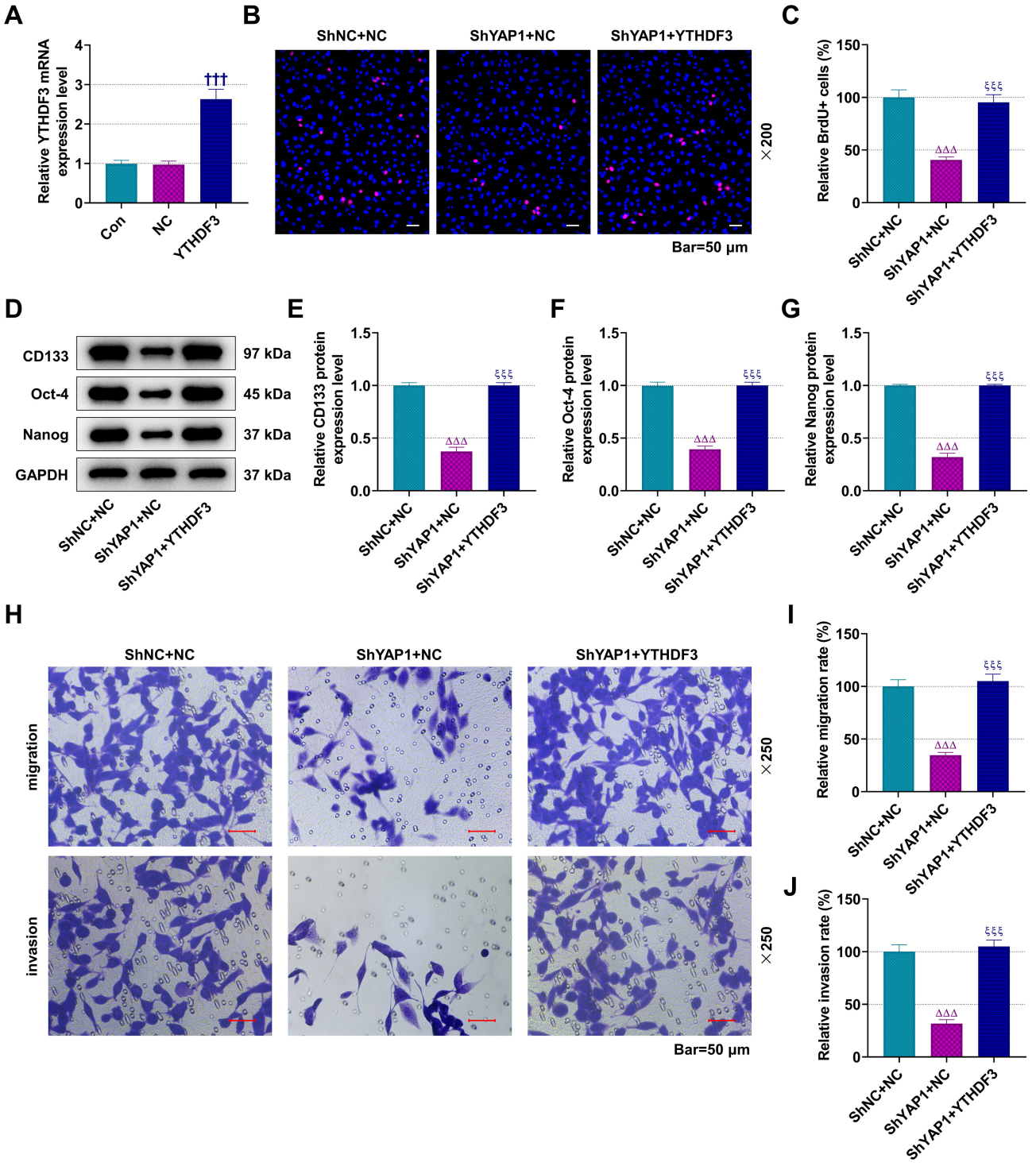

Fig. 5. YAP1 knockdown-induced inhibition on cell growth/migration/invasion/stemness maker expression levels in BCSCs was reversed by YTHDF3 overexpression. (A) qRT-PCR was performed to determine *YTHDF3* mRNA expression in BCSCs and *GAPDH* served as an internal control. (B,C) BrdU assay was conducted for the assessment of BCSC proliferation (magnification × 200, scale bar = 50 μm). (D–G) Protein levels of CD133, Oct-4 and Nanog in BCSCs were measured by Western blot assay and normalized to GAPDH. (H–J) Transwell assay was carried out for the analyses on the migration and invasion of BCSCs (magnification × 250, scale bar = 50 μm). Con group: normal BCSCs; NC group: NC-transfected BCSCs; Sh*YAP1* group: Sh*YAP1*-transfected BCSCs; YTHDF3 group: YTHDF3 overexpression plasmid-transfected BCSCs; ShNC+NC group: BCSCs co-transfected with ShNC and NC; Sh*YAP1*+YTHDF3 group: BCSCs co-transfected with Sh*YAP1* and YTHDF3 overexpression plasmid. †vs. NC, $^{\triangle}$vs. ShNC+NC, $^{\xi}$vs. Sh*YAP1*+NC: $^{\dagger\dagger\dagger}p < 0.001$, $^{\triangle\triangle\triangle}p < 0.001$, $^{\xi\xi\xi}p < 0.001$. n = 3.

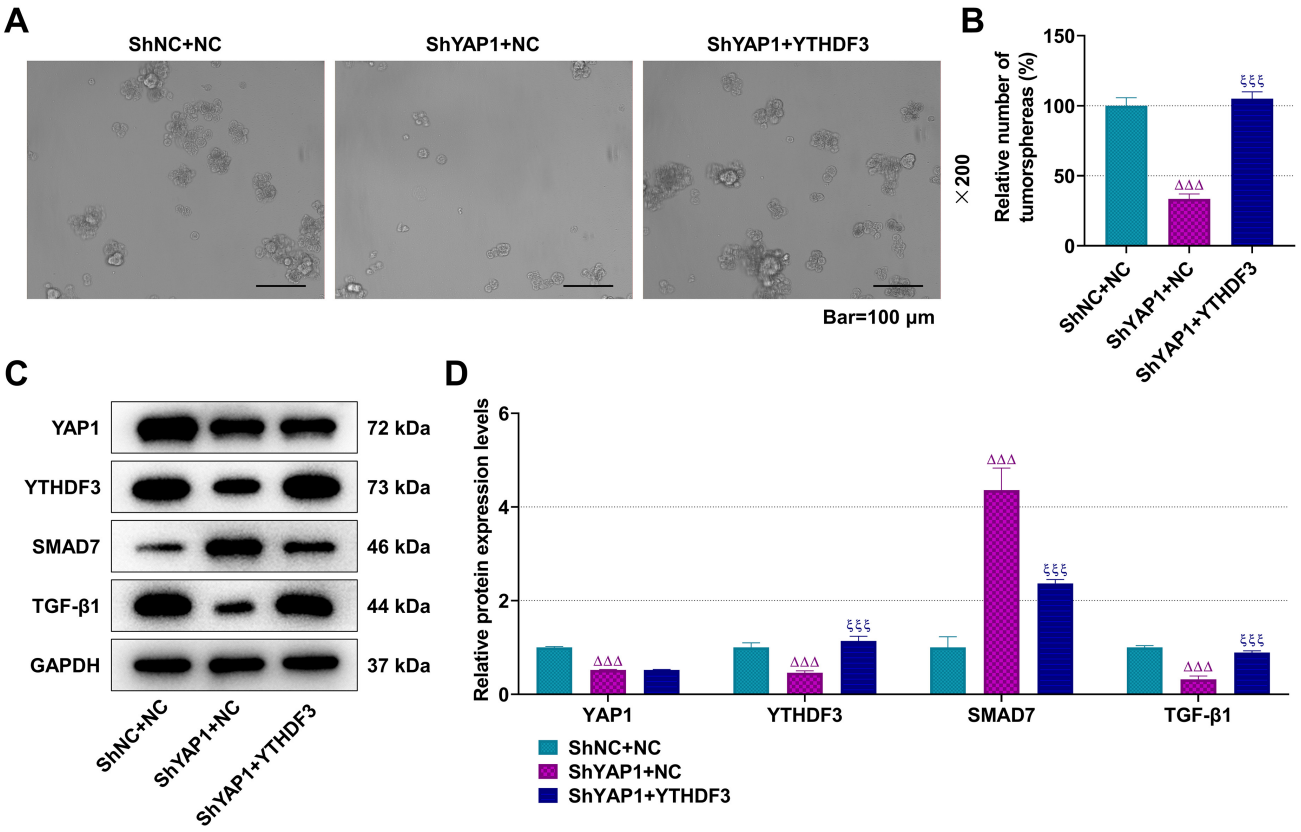

Fig. 6. Effects of YAP1 knockdown on tumour sphere formation as well as YTHDF3, TGF-β1 and *SMAD7* expression levels in BCSCs were negated by YTHDF3 overexpression. (A,B) Imagines of tumour spheres in BCSCs (magnification × 200, scale bar = 100 μm) and the number of tumor spheres were counted. (C,D) Protein levels of YAP1/YTHDF3/*SMAD7*/TGF-β1 in BCSCs were measured by Western blot assay and normalized to GAPDH. Sh*YAP1* group: Sh*YAP1*-transfected BCSCs; ShNC+NC group: BCSCs co-transfected with ShNC and NC; Sh*YAP1*+YTHDF3 group: BCSCs co-transfected with Sh*YAP1* and YTHDF3 overexpression plasmid. $^{\triangle}$vs. ShNC+NC, $^{\xi}$vs. Sh*YAP1*+NC: $^{\triangle\triangle\triangle}p < 0.001$, $^{\xi\xi\xi}p < 0.001$. n = 3.

Discussion

Tumor recurrence and drug resistance pose significant challenges in the treatment of BLCA, with CSCs playing a pivotal role in tumor metastasis and resistance to conventional therapies [22]. Therefore, identifying novel targets against BCSCs is imperative. This study elucidated that knockdown of YAP mitigated the malignant characteristics of BCSCs.

CSCs are notorious for driving tumour recurrence due to their resistance to traditional chemotherapy, attributed to heightened DNA damage response activities [20]. Given their pivotal role in cancer initiation, metastasis and relapse of cancer, targeting the self-renewal of CSCs is a potential approach for cancer treatment [23]. BCSCs, renowned stemness properties and self-renewal capacity, exemplify this paradigm through their ability to form tumour spheres [24]. Makers like CD133, Oct-4 and Nanog play pivotal roles in identifying CSCs [25]. CD133 serves as a hallmark of stemness in various cancers and CD133^{+} BCSCs are associated with aggressive tumorigenicity in BLCA [26]. Oct-4 is a modulator of CSC self-renewal and its expression is positively correlated with advanced tumour grade and recurrence in BLCA [25]. High Nanog expression has been found in BLCA, which indicates poor overall survival and recurrence-free survival of BLCA patients [27]. Our study demonstrates that BCSCs exhibit high CD133^{+} phenotype, express CSC-related marker proteins, and display enhanced invasion, migration and tumour sphere formation capabilities, affirming the unfavourable characteristics of BCSCs in BLCA progression.

YAP1 has emerged as an oncogene in various cancers, with elevated expression particularly noted in advanced and metastatic BLCA [28]. Its overexpression has been linked to the promotion of proliferation and invasion of BLCA cells [29], while YAP1 silencing has been shown to enhance drug sensitivity and induce cell apoptosis, along with reducing cell viability and migration in chemoresistant BLCA cells [30]. Moreover, YAP1 is highly expressed in BCSCs and is required to confer self-renewal properties to BCSCs [30]. Previous study has shown that YAP1 interacts with cyclooxygenase 2 for the maintenance and propagation of BCSCs, and blocking these pathways can improve long-term efficacy by reducing therapeutic resistance [31]. Sun

et al. [32] found that YAP1 inhibitors decrease Oct-4 and Nanog expression levels in breast cancer cells. YAP1 also increases the ratio of $CD133^+$ cells in small-cell lung cancer, which further results in the radiation resistance of cancer cells [33]. Consistent with these findings, our study revealed high YAP1 expression in BCSCs, and knockdown of YAP1 suppressed the malignant behaviors of BCSCs while downregulating CSC biomarker expression levels. These results underscore the positive regulatory role of YAP1 in BCSC stemness.

Previous studies have documented that YAP1 can upregulate m6A reader YTHDF3, leading to GAS5 degradation, and promoting the progression of colorectal cancer [34], highlighting the significance of YAP1-YTHDF3 signaling pathway in cancer development. YTHDF3 has been implicated in facilitating the translation of integrin alpha-6, thereby promoting the growth and development of BLCA cells [8]. Additionally, it has been shown to promote migration, invasion and EMT of triple-negative breast cancer cells [35]. Consistent with these findings, our study demonstrated that YTHDF3 levels were downregulated by Sh*YAP1*, while YTHDF3 overexpression reversed the inhibitory effect of Sh*YAP1* on BCSC-induced stemness. This effect may be attributed to YTHDF3-mediated modulation of m6A-methylated gene expression levels [8]. According to the analysis of genes associated with BLCA and YAP1, we chose *SMAD7* as the target gene in the following studies. Knockdown of m6A reader YTHDF2 has been reported to promote the stability and expression of *SMAD7* [36] while YTHDF3 acts as a co-factor to accelerate YTHDF2-induced decay of m6A-containing mRNAs [37]. The present study found that inhibition of YAP1 decreased *SMAD7* m6A level and weakened the YTHDF3-*SMAD7* interaction in BCSCs, suggesting the positive regulation of YAP1 on the interaction between YTHDF3 and m6A-modified *SMAD7*.

In BLCA, EMT plays a crucial role in enabling tumor cells to acquire CSC characteristics, characterized by heightened proliferation and invasion capabilities [38]. TGF-β1 is known to promote tumor invasion and metastasis by inducing EMT [39]. Specifically in BLCA, TGF-β1 has been implicated in fostering cancer cell stemness and chemoresistance, with inhibition of TGF-β1 leading to a decrease in BCSCs [40]. *SMAD7* serves as an antagonist of the TGF-β signaling pathway, and its upregulation can inhibit tumor growth and metastasis in BLCA by blocking the TGF-β cascade [41]. Evidence suggests that increased mRNA expression and enhanced stability of *SMAD7* in cancers can be attributed to various modification mechanisms [42]. The methylation of *SMAD7* is known to activate the TGF-β signaling, which further promotes EMT and cancer stem-cell formation [43]. The degradation of *SMAD7* induced by m6A writer *METTL3* is associated with aggressive phenotypes of cancer cells in colorectal cancer [18] while stabilizing *SMAD7* can prevent TGF-β-induced cancer stemness and metastasis in breast cancer [44]. In lung cancer, the decay of *SMAD7* facilitates cancer cell migration and invasion by enhancing TGF-β-dependent EMT signaling [45]. In this study, upregulation of TGF-β1 and downregulation of *SMAD7* were found in BCSCs, whereas their expression levels were negatively or positively regulated by Sh*YAP1* and further reversed by YTHDF3 overexpression. Taken together, YAP1 knockdown inhibits YTHDF3-induced decay of m6A-methylated *SMAD7*, which further blocks the TGF-β1 pathway and consequently improves BCSC stemness. However, the identification of precise modification site is crucial for understanding the underlying mechanism of YAP1 knockdown on inhibiting BCSC stemness, which will be investigated in our future study.

Conclusion

In conclusion, our study elucidates that knockdown of YAP1 impedes YTHDF3-induced degradation of m6A-methylated *SMAD7*, consequently inhibiting BCSC stemness. Targeting YAP1 presents a promising avenue for enhancing the prognosis of BLCA following surgery, and it may be a novel treatment target for BLCA. However, this study solely focused on YAP knockdown to investigate its impact on BCSC stemness. Future research will explore the consequences of YAP1 overexpression on BCSC stemness. Moreover, subsequent studies will aim to dissect the complex interactions between YAP1, YTHDF3, and *SMAD7*, as well as other potential regulatory factors and signaling pathways implicated in BLCA.

Availability of Data and Materials

The analyzed data sets generated during the study are available from the corresponding author on reasonable request.

Author Contributions

Substantial contributions to conception and design: DDQ; data acquisition, data analysis and interpretation: LLG, XWY; drafting the article or critically revising it for important intellectual content: all authors; final approval of the version to be published: all authors; agreement to be accountable for all aspects of the work in ensuring that questions related to the accuracy or integrity of the work are appropriately investigated and resolved: all authors.

Ethics Approval and Consent to Participate

Not applicable.

Acknowledgment

Not applicable.

Funding

This work was supported by Zhejiang Province Medical and Health Science and Technology Plan Project [No. 2021RC096] and Zhejiang Traditional Chinese Medicine Science and Technology Plan Project [No. 2023ZL370].

Conflict of Interest

The authors declare no conflict of interest.

Supplementary Material

Supplementary material associated with this article can be found, in the online version, at https://doi.org/10.24976/Discov.Med.202436186.138.

References

[1] Dobruch J, Oszczudłowski M. Bladder Cancer: Current Challenges and Future Directions. Medicina. 2021; 57: 749.

[2] Abbaoui B, Lucas CR, Riedl KM, Clinton SK, Mortazavi A. Cruciferous Vegetables, Isothiocyanates, and Bladder Cancer Prevention. Molecular Nutrition & Food Research. 2018; 62: e1800079.

[3] Zhan Y, Chen Z, He S, Gong Y, He A, Li Y, *et al*. Long non-coding RNA SOX2OT promotes the stemness phenotype of bladder cancer cells by modulating SOX2. Molecular Cancer. 2020; 19: 25.

[4] Aghaalikhani N, Rashtchizadeh N, Shadpour P, Allameh A, Mahmoodi M. Cancer stem cells as a therapeutic target in bladder cancer. Journal of Cellular Physiology. 2019; 234: 3197–3206.

[5] Pan S, Zhan Y, Chen X, Wu B, Liu B. Identification of Biomarkers for Controlling Cancer Stem Cell Characteristics in Bladder Cancer by Network Analysis of Transcriptome Data Stemness Indices. Frontiers in Oncology. 2019; 9: 613.

[6] Qin S, Mao Y, Wang H, Duan Y, Zhao L. The interplay between m6A modification and non-coding RNA in cancer stemness modulation: mechanisms, signaling pathways, and clinical implications. International Journal of Biological Sciences. 2021; 17: 2718–2736.

[7] Uddin MB, Wang Z, Yang C. The m^6A RNA methylation regulates oncogenic signaling pathways driving cell malignant transformation and carcinogenesis. Molecular Cancer. 2021; 20: 61.

[8] Jin H, Ying X, Que B, Wang X, Chao Y, Zhang H, *et al*. N^6-methyladenosine modification of ITGA6 mRNA promotes the development and progression of bladder cancer. eBioMedicine. 2019; 47: 195–207.

[9] Yu Y, Su X, Qin Q, Hou Y, Zhang X, Zhang H, *et al*. Yes-associated protein and transcriptional coactivator with PDZ-binding motif as new targets in cardiovascular diseases. Pharmacological Research. 2020; 159: 105009.

[10] Chen X, Li S, Yu Z, Tan W. Yes-associated protein 1 promotes bladder cancer invasion by regulating epithelial-mesenchymal transition. International Journal of Clinical and Experimental Pathology. 2019; 12: 1070–1077.

[11] Islam SS, Mokhtari RB, Noman AS, Uddin M, Rahman MZ, Azadi MA, *et al*. Sonic hedgehog (Shh) signaling promotes tumorigenicity and stemness via activation of epithelial-to-mesenchymal transition (EMT) in bladder cancer. Molecular Carcinogenesis. 2016; 55: 537–551.

[12] Yu H, Hou Z, Chen N, Luo R, Yang L, Miao M, *et al*. Yes-associated protein contributes to magnesium alloy-derivedinflammation in endothelial cells. Regenerative Biomaterials. 2022; 9: rbac002.

[13] Yuan F, Yin H, Deng Y, Jiao F, Jiang H, Niu Y, *et al*. Overexpression of Smad7 in hypothalamic POMC neurons disrupts glucose balance by attenuating central insulin signaling. Molecular Metabolism. 2020; 42: 101084.

[14] Hao Y, Baker D, Ten Dijke P. TGF-β-Mediated Epithelial-Mesenchymal Transition and Cancer Metastasis. International Journal of Molecular Sciences. 2019; 20: 2767.

[15] Ren L, Jiang M, Xue D, Wang H, Lu Z, Ding L, *et al*. Nitroxoline suppresses metastasis in bladder cancer via EGR1/circNDRG1/miR-520h/smad7/EMT signaling pathway. International Journal of Biological Sciences. 2022; 18: 5207–5220.

[16] Ma L, Jiang H, Xu X, Zhang C, Niu Y, Wang Z, *et al*. Tanshinone IIA mediates SMAD7-YAP interaction to inhibit liver cancer growth by inactivating the transforming growth factor beta signaling pathway. Aging. 2019; 11: 9719–9737.

[17] Zhang Y, Gu X, Li D, Cai L, Xu Q. METTL3 Regulates Osteoblast Differentiation and Inflammatory Response via Smad Signaling and MAPK Signaling. International Journal of Molecular Sciences. 2019; 21: 199.

[18] Chen W, Wang H, Mi S, Shao L, Xu Z, Xue M. ALKBH1-mediated m^1 A demethylation of METTL3 mRNA promotes the metastasis of colorectal cancer by downregulating SMAD7 expression. Molecular Oncology. 2023; 17: 344–364.

[19] Ni W, Yao S, Zhou Y, Liu Y, Huang P, Zhou A, *et al*. Long noncoding RNA GAS5 inhibits progression of colorectal cancer by interacting with and triggering YAP phosphorylation and degradation and is negatively regulated by the m^6A reader YTHDF3. Molecular Cancer. 2019; 18: 143.

[20] Shi X, Chen S, Zhang Y, Xie W, Hu Z, Li H, *et al*. Norcantharidin inhibits the DDR of bladder cancer stem-like cells through cdc6 degradation. OncoTargets and Therapy. 2019; 12: 4403–4413.

[21] Sun X, Song J, Li E, Geng H, Li Y, Yu D, *et al*. Cigarette smoke supports stemness and epithelial-mesenchymal transition in bladder cancer stem cells through SHH signaling. International Journal of Clinical and Experimental Pathology. 2020; 13: 1333–1348.

[22] Luo Y, Tian Z, Hua X, Huang M, Xu J, Li J, *et al*. Isorhapontigenin (ISO) inhibits stem cell-like properties and invasion of bladder cancer cell by attenuating CD44 expression. Cellular and Molecular Life Sciences. 2020; 77: 351–363.

[23] Chen X, Xie R, Gu P, Huang M, Han J, Dong W, *et al*. Long Noncoding RNA *LBCS* Inhibits Self-Renewal and Chemoresistance of Bladder Cancer Stem Cells through Epigenetic Silencing of SOX2. Clinical Cancer Research. 2019; 25: 1389–1403.

[24] Xu R, Zhu X, Chen F, Huang C, Ai K, Wu H, *et al*. LncRNA XIST/miR-200c regulates the stemness properties and tumourigenicity of human bladder cancer stem cell-like cells. Cancer Cell International. 2018; 18: 41.

[25] Abugomaa A, Elbadawy M, Yamawaki H, Usui T, Sasaki K. Emerging Roles of Cancer Stem Cells in Bladder Cancer Progression, Tumorigenesis, and Resistance to Chemotherapy: A Potential Therapeutic Target for Bladder Cancer. Cells. 2020; 9: 235.

[26] Farid RM, Sammour SAE, Shehab ElDin ZA, Salman MI, Omran TI. Expression of CD133 and CD24 and their different phenotypes in urinary bladder carcinoma. Cancer Management and Research. 2019; 11: 4677–4690.

[27] Siddiqui Z, Srivastava AN, Sankhwar SN, Dalela D, Singh V, Zaidi N, *et al*. Synergic effects of cancer stem cells markers, CD44 and embryonic stem cell transcription factor Nanog, on bladder cancer prognosis. British Journal of Biomedical Science. 2020; 77: 69–75.

[28] Xia J, Zeng M, Zhu H, Chen X, Weng Z, Li S. Emerging role of

Hippo signalling pathway in bladder cancer. Journal of Cellular and Molecular Medicine. 2018; 22: 4–15.

[29] Dong L, Lin F, Wu W, Liu Y, Huang W. Verteporfin inhibits YAP-induced bladder cancer cell growth and invasion via Hippo signaling pathway. International Journal of Medical Sciences. 2018; 15: 645–652.

[30] Zhao AY, Dai YJ, Lian JF, Huang Y, Lin JG, Dai YB, *et al*. YAP regulates ALDH1A1 expression and stem cell property of bladder cancer cells. OncoTargets and Therapy. 2018; 11: 6657–6663.

[31] Ooki A, Del Carmen Rodriguez Pena M, Marchionni L, Dinalankara W, Begum A, Hahn NM, *et al*. YAP1 and COX2 Coordinately Regulate Urothelial Cancer Stem-like Cells. Cancer Research. 2018; 78: 168–181.

[32] Sun HL, Men JR, Liu HY, Liu MY, Zhang HS. FOXM1 facilitates breast cancer cell stemness and migration in YAP1-dependent manner. Archives of Biochemistry and Biophysics. 2020; 685: 108349.

[33] Yang K, Zhao Y, Du Y, Tang R. Evaluation of Hippo Pathway and CD133 in Radiation Resistance in Small-Cell Lung Cancer. Journal of Oncology. 2021; 2021: 8842554.

[34] Liu S, Li G, Li Q, Zhang Q, Zhuo L, Chen X, *et al*. The roles and mechanisms of YTH domain-containing proteins in cancer development and progression. American Journal of Cancer Research. 2020; 10: 1068–1084.

[35] Lin Y, Jin X, Nie Q, Chen M, Guo W, Chen L, *et al*. YTHDF3 facilitates triple-negative breast cancer progression and metastasis by stabilizing ZEB1 mRNA in an m^6A-dependent manner. Annals of Translational Medicine. 2022; 10: 83.

[36] Zhang D, Ning J, Okon I, Zheng X, Satyanarayana G, Song P, *et al*. Suppression of m6A mRNA modification by DNA hypermethylated ALKBH5 aggravates the oncological behavior of KRAS mutation/LKB1 loss lung cancer. Cell Death & Disease. 2021; 12: 518.

[37] Chen J, Tian Y, Zhang Q, Ren D, Zhang Q, Yan X, *et al*. Novel Insights Into the Role of N6-Methyladenosine RNA Modification in Bone Pathophysiology. Stem Cells and Development. 2021; 30: 17–28.

[38] Zhang Y, Zhang X, Huang X, Tang X, Zhang M, Li Z, *et al*. Tumor stemness score to estimate epithelial-to-mesenchymal transition (EMT) and cancer stem cells (CSCs) characterization and to predict the prognosis and immunotherapy response in bladder urothelial carcinoma. Stem Cell Research & Therapy. 2023; 14: 15.

[39] Papoutsoglou P, Moustakas A. Long non-coding RNAs and TGF-β signaling in cancer. Cancer Science. 2020; 111: 2672–2681.

[40] Zhuang J, Shen L, Yang L, Huang X, Lu Q, Cui Y, *et al*. TGFβ1 Promotes Gemcitabine Resistance through Regulating the LncRNA-LET/NF90/miR-145 Signaling Axis in Bladder Cancer. Theranostics. 2017; 7: 3053–3067.

[41] An M, Zheng H, Huang J, Lin Y, Luo Y, Kong Y, *et al*. Aberrant Nuclear Export of circNCOR1 Underlies SMAD7-Mediated Lymph Node Metastasis of Bladder Cancer. Cancer Research. 2022; 82: 2239–2253.

[42] Tian H, Liu C, Yu J, Han J, Du J, Liang S, *et al*. PHF14 enhances DNA methylation of SMAD7 gene to promote TGF-β-driven lung adenocarcinoma metastasis. Cell Discovery. 2023; 9: 41.

[43] Katsuno Y, Qin J, Oses-Prieto J, Wang H, Jackson-Weaver O, Zhang T, *et al*. Arginine methylation of SMAD7 by PRMT1 in TGF-β-induced epithelial-mesenchymal transition and epithelial stem-cell generation. The Journal of Biological Chemistry. 2018; 293: 13059–13072.

[44] Han S, Wang R, Zhang Y, Li X, Gan Y, Gao F, *et al*. The role of ubiquitination and deubiquitination in tumor invasion and metastasis. International Journal of Biological Sciences. 2022; 18: 2292–2303.

[45] Tong L, Shen S, Huang Q, Fu J, Wang T, Pan L, *et al*. Proteasome-dependent degradation of Smad7 is critical for lung cancer metastasis. Cell Death and Differentiation. 2020; 27: 1795–1806.